Effect of Sulfides on Welds Between Ni Alloys and Free Machining Steel

Joint strengths rise and fall with energy input, but the controlling factors are particle count and amount of interdiffusion

BY P. J. McWEENY AND B. GREGORY

ABSTRACT. Samples of three nickel base alloys have been resistance welded to a free machining steel (AISI C1213 modified) using a commercial automatic machine. As a function of welding input energy the factors contributing to weld strength have been determined by mechanical testing and metallographic techniques with particular reference to the role of sulfides. In general, the least number of precipitated particles gave the strongest welds provided adequate interdiffusion of the elements present in the materials had taken place.

Introduction

It is necessary in the manufacture of certain engineering components to produce strong welds between apparently incompatible materials. Generally, free machining steel is obtainable in large commercial quantities and is useful for its preforming and machining properties, whereas the nickel base alloys considered here are generally much more expensive, but have good corrosion and heat resistant properties.

Therefore for components which may be used in gas ignition systems it is very desirable that the welds produced, often at high production rates, between such semi-incompatible materials, be strong and free from failure at high temperatures in essentially hostile environments.

Consequently the purpose of this paper is to show how some of the metallurgical variables involved in the commercial production of such components can be assessed in relation to the formation of satisfactory welds.

Previous Work

Any reference in the literature to the welding of the materials used in this investigation could not be found. However, information concerning the behavior of sulfur in the presence of iron, nickel, titanium, carbon and manganese could be deduced from phase diagrams by Hanson (Ref. 1) and by reference to the standard free energies of formation (Δ G°k cal) of various sulfides as a function of temperature (Ref. 2).

The presence of sulfur is known to cause embrittlement problems in the welding and casting of ferrous materials and so some knowledge and understanding of the occurrence and forms the element would take in this particular investigation is important to the production of satisfactory welds. The morphology of sulfide inclusions in steel depends upon the steelmaking practice from which three types are possible according to Sims (Ref. 3); namely, randomly dispersed globular forms, chain-like distributions and angular inclusions randomly dispersed.

The production of the globular or chain-like forms is dependent upon oxygen content, but the angular variety is to be expected when aluminim, carbon, silicon, phosphorus or chromium are present. Steels which are deoxidized, but without excess deoxidant, have a high sulfur solubility and so the sulfide phase precipitates late in the solidification process at the grain boundaries. When the angular sulfides are formed the steel has a lower sulfur solubility, and the inclusion is precipitated before the chain-like forms and is randomly dispersed (Refs. 4,5).

Manganese sulfide can also absorb considerable amounts of other transition metals into substitutional solid solutions producing sulfides of the type (Mn X)S. This can be as much as 60-70 wt% for chromium and about 15 wt% for nickel (Ref. 6) both of which are elements present in the commercial materials to be used in this investigation and so could have a significant role in the welding process.

Previous practical experience of welding such materials has been limited. In this sense it had been noted that weld quality was some function of energy input, and the weld quality was assessed in a crude manner by attempting to pull apart small welded components with a pair of pliers. This served as a rapid

The authors are associated with the Department of Mechanical Engineering, University of Salford, Salford, England.

method for determining good and poor welds but the test also revealed a number of different fracture types, namely:

1. a "hot-stick" type of fracture where both materials seemed to be largely unaffected by interpenetration,
2. a "body pull-out" type where a large nugget of steel adhered to the nickel base wire and the fracture surface appeared crystalline.
3. a "nickel base wire" fracture in which the weakest component was the wire some distance from the weld,
4. a "weld-line" failure in which fracture occurred within the fusion zone of the weld.

It was therefore considered necessary to investigate the factors which led to failure but, when controlled, could lead to optimum production of a strong satisfactory weldment.

Experimental

In view of the fracture types produced from the crude test, it was thought that a more quantitative determination of the energy input versus weld strength relationship would determine the course of investigation. The automatic welding machine used in the tests was a development of (Agnew and Slee) automatic welding machines hitherto used for high speed welding situations and had provision for the control of transformer tapping, force and weld time. These were selected to operate at values of no. 5 (tap), 100 lb (force) and 8 cycles at 50 cps (time), respectively. The welding energy units recorded are a function of the product of welding current and voltage integrated with respect to time.

Mechanical Testing

Because sawtooth jaws cut easily into the nickel base materials with subsequent weakening, tensile testing was not a feasibility, and so a small shear testing rig was devised. Flat jaws were used so that the nickel base alloys were sheared very near to the weld interface in all cases. The applied force was also made parallel to the axis of pull so that tearing effects could be minimized. The method gave consistent results for welds produced under the same conditions and was therefore used as a measure of weld strength.

Materials and Specimens

The analysis and properties of the materials used in the investigation are shown in Tables 1 and 2 respectively. The modified steel (AISI C1213) was available in bulk form and the nickel base alloys in the form of wire of approximately 0.080 in. diameter. Both fractured and unfractured weld assemblies were examined using optical microscopy. High magnifications were required in order to examine the small width of some of the fusion zones (about 10^{-3} mm). In order to minimize the formation of oxide films between final polishing and etching, specimens were stored in methanol. The etching process required some care and development in order that a similar level of attack would occur on the steel, the highly resistant nickel base materials and the weld zones. Because of the natural galvanic action of the assembly, electrolytic etching techniques were utilized. These used combinations of nitric and hydrochloric acids in ethyl and methyl alcohol. It was found that acid concentrations were critical to 1 drop per 50 cc of solvent. Those found to be most suitable are shown in Table 3.

Tables 1 — Chemical Composition of Materials Used in This Study

Element	AISI C1213 modified	Nickel base (wire) materials S4P	Nirex	2S5
Carbon	0.10 max	0.07 max	0.07 max	—
Sulfur	0.30-0.38	—	—	0.1 max
Manganese	0.90-1.20	3.75-4.25	0.50 max	2.5-3.5
Silicon	0.002-0.02	0.9-1.1	0.50 max	1.5-2.0
Iron	Bal	0.40 max	6.0-8.0	0.50 max
Nickel	—	Bal	Bal	Bal
Chromium	—	0.1 max	14.0-16.0	4.5-5.5
Trace	—	Mg, Zr, Ti, Cu	Mg, Cu, Zr, Ti	Cu, Mg, Ti, Zr

Table 2 — Properties of Nickel Base Materials Used in This Study

Nickel base material	Y.S., ton/in.^{2}	U.T.S., ton/in.^{2}	Elong., %
S4P	13.1	32.3	41.5
Nirex (normal anneal)	18.7	39.3	40.0
Nirex (double anneal)	18.3	37.3	41.0
2S5 (normal anneal)	17.0	36.5	42.5
2S5 (double anneal)	16.6	35.6	43.0

Table 3 — Electrolytic Etching Formulations

Chemical	Nirex	S4P	2S5
Ethanal, cc	100	25	100
Methanol, cc	—	75	—
HNO_3, drops	8	10	15
HCl, drops	—	3	—
Voltage, V	7	10	10

For the unfractured specimens the weld interfaces were examined at high magnification (X3000) and note taken of the following:

1. the degree of liquation that had occured at the interface and grain boundaries,
2. the evidence of sulfide phase formation from the MnS inclusions present in the steel, and
3. the evidence of other interfacial alloying.

In order to prevent damage to the fracture surfaces of sheared specimens, samples were nickel plated before grinding and polishing.

Electron Microscopy and Microanalysis

The fracture surfaces of the weld sections were examined by electron microscopy and scanning electron microscopy. In the former both plastic and carbon extraction replicas were used. Some difficulty was experienced in taking plastic replicas because the fracture surfaces were generally small and burred and tended to be craterous. Photographs were taken where appropriate and extracted particles analyzed using the x-ray Laue method. The topography of the centers of fractured welds were also examined using a scanning microscope.

The distribution of the various elements across the weld interfaces was

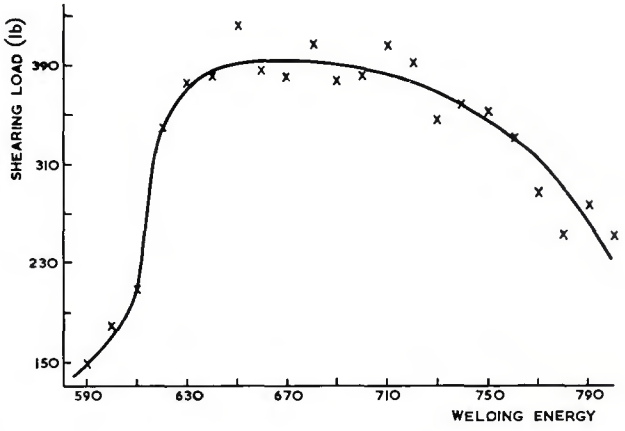

Fig. 1 — Shearing load versus welding energy for welds with S4P nickel base alloy. Types of failure varied with increasing energy ranges as follows: 580-600, 'hot stick' fracture; 600-630, 'body pull out' fracture; 630-700, 'nickel base wire' failure; 700-740, 'mixed wire and weld line' failure; 740-800, 'weld line' failure

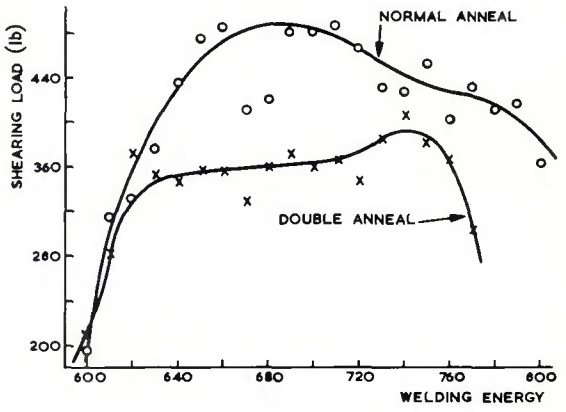

Fig. 2 — Shearing load versus welding energy for welds with Nirex

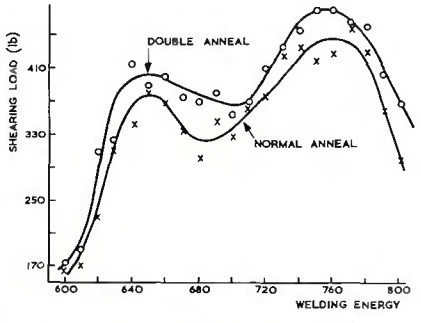

Fig. 3 — Shearing load versus welding energy for welds with 2S5 nickel base alloy

examined using electron probe microanalysis. Scans for sulfur, chromium, nickel, manganese and iron were made in an attempt to relate the extent of interdiffusion between the steel and nickel base alloys to the input energy, and hence to relate this to weld strengths. Because of operating diffuclties however, this was only semi-quantitative but asslsted in obtaining a qualitative appreciation.

Results and Discussion

The shearing load versus welding energy curves for the wires S4P, Nirex and 2S5 are shown in Figs. 1, 2 and 3. It can be seen that some scatter in the average shear load values occurred. Although larger batch sizes may have helped to reduce this, the chief sources of error are attributed to the testing method, welding machine instability and nonhomogeneity of the materials. In general the load required to shear the welds increased rapidly with increasing weld energy to an approximate plateau value and then rapidly decreased. In the case of the double annealed Nirex and the 2S5 wires in two different states of anneal, there is a tendency towards a secondary effect which further increases weld strength. This can be attributed to a degree of mutual solubility which would relate to the depth of weld zone, and also to a redistribution or reduction of sulfide particles at the interfaces. See Fig. 4.

The apparent fracture types described earlier progressed in the same order as that found in the crude tests. The range of welding energies over which these occurred for the S4P alloy is shown in Fig. 1. Nirex in the normal annealed state appears to be the best welding material but since the physical properties of the two annealed states were only slightly different (see Table 2) the curves in Fig. 2 should be viewed with some caution. It is here suggested that

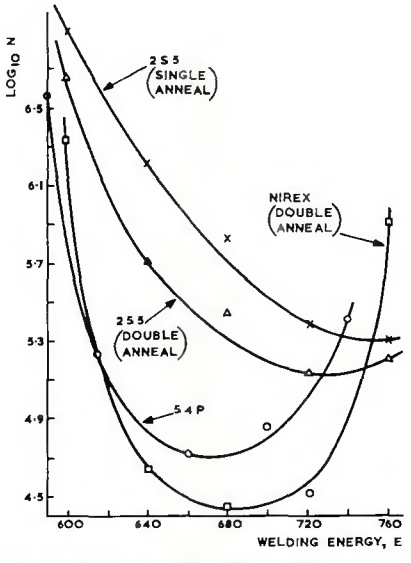

Fig. 4 — Number N of MnS particles/mm² on fracture surfaces versus welding energy

welding machine instability or slightly different operating conditions may be the real cause of this effect, especially if one considers the curves for 2S5 In Fig. 3. In this case small differences in physical properties merely displaced the curve by about 30 lb without significant alteration of the characteristic, and so it would appear that no general rule exists for the effects of physical condition on the weldability of the nickel base alloys.

In general the metallography of all the unsheared welds appeared similar at low magnification, except that the depths of the heat-affected zones increased with increasing weld energy. This was to be expected and the relationship held true for all the nickel base alloys. Examination at higher magnifications also revealed that for all the materials manganese sulfide tended to spheroidize with increasing input energy, except in the case of the Nirex welds where it tended to become elongated and penetrate the intergranular and interfacial regions. Towards the upper end of weld input energies used more spheroidization of MnS occurred, with sometimes smaller reprecipitated spheroids being formed in the region of the original MnS constituent of the steel. This was accompanied by a tendency for cracking and hot tearing to occur along the weld interface for the Nirex welds and for the formation of second phases to appear. These interfacial second phases were dendritic in form for the 2S5 welds, when viewed under the microscope.

To some extent this was to be expected from the theory and knowledge that MnS has a low softening and melting temperature compared with the other metallic constituents. In addition, the elements such as nickel and chromium in the wires would tend to alloy with the steel, and any excess

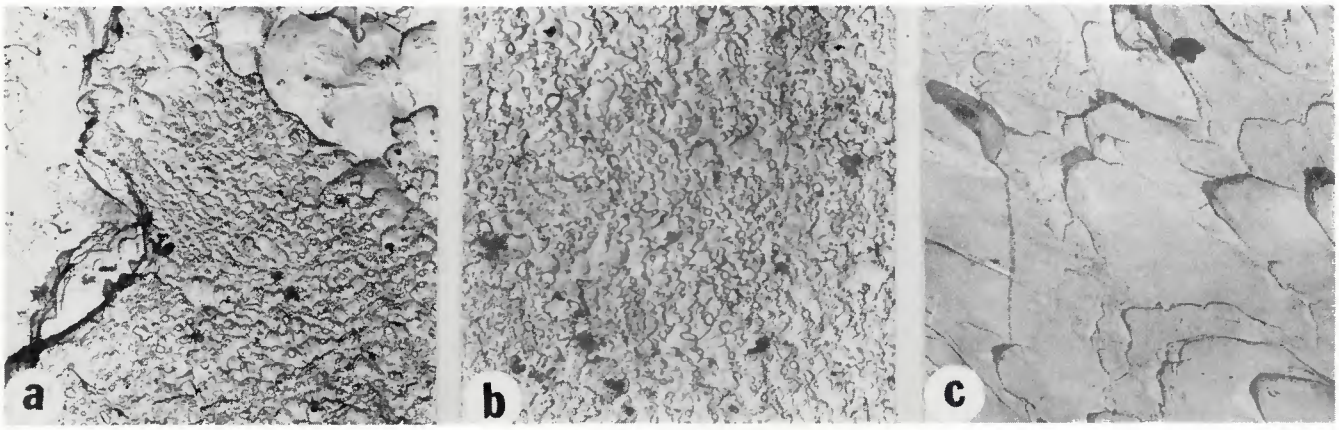

Fig. 5 — Electron photomicrographs showing manganese sulfide particle coarsening with increasing input energy (a) to (c). X4000, not reduced

of manganese and sulfur would tend to combine preferentially — in agreement with the lower changes of free energy of formation — compared with the formation of other possible sulfides, notably those of iron, nickel, chromium and silicon.

In the case of the sheared welds metallographic examination revealed that, where MnS extended only to the interface, fracture occurred within the body steel, but where it entered the weld zone, fracture tended to take place in the nickel based materials. Electron micrographs obtained from replicas of the fracture surfaces showed that welds tended to fail by ductile fracture initiated by small, well dispersed particles. These photographs also revealed that at low input energies the particles were very small and finely dispersed. With increasing input energy they coarsened and their number decreased until, under conditions of overwelding, the number decreased again but now the particle size was greater than was the case for low energy input welds. This effect is shown in Fig. 5(a), (b) and (c) for S4P wire, the trends being similar for the other nickel base wire materials.

X-ray diffraction conducted on the extracted particles proved that these particles were α − MnS, but in the case of Nirex and the 2S5 welds, where second phase particles appeared in the grain boundaries of the wire, a similar analysis showed them to be the complex sulfide $(Ti\ Fe)_4C_2S_2$.

Scanning electron micrographs and the particle analysis agreed with the results obtained from electron microscopy. Using these techniques it was easy to determine the number of particles per unit area by using a suitable grid. The particle count results were seen to vary as a function of the input energy for each wire material used and by using Figs. 1, 2 and 3 could be related to the fracture load. These results are shown in Figs. 4 and 6. Generally the trend was the same for all the nickel base materials used, namely that the number of particles decreased to a minimum with increasing input energy and then increased again. The photographs in Fig. 7 (a-e) show scanning electron micrographs of this effect for the Nirex welds produced at 600, 640, 680, 720 and 760 energy units respectively. However, low energy welds on 2S5 exhibited different fracture surfaces for the single and double annealed states, Fig. 8(a) and (b), but the fractures became similar in appearance at high input energies, Fig. 8(c) and (d).

The optical and electron microscopy conducted on all these samples showed that where a manganese sulfide inclusion is exposed at the weld interface, low melting point compounds can be formed which spread along the interface and penetrate the grain boundaries. This is important where weld strength is concerned since the incidence of these compounds is related to the surface area of manganese sulfide presented at the interface. This will depend upon the concentration and the aspect ratio (ratio of length to diameter) of MnS inclusions in the steel. Weld strength would then tend to fall with increasing sulfur content and aspect ratio. A small aspect ratio of about 5 is considered beneficial for machinability purposes.

Microprobe analysis showed that the interdiffusion of elements tended to increase with energy input but there was no evidence of sulfur diffusion as such. This implied that the sulfur present remained as discrete particles even though their number and size changed with input energy. Those small amounts which did diffuse or react with elements of the wire materials, formed complex particles such as $(Fe, Ti)_4C_2S_2$ as in the Nirex welds. These tended to cause embrittlement in the nickel base materials and hence influence the value at

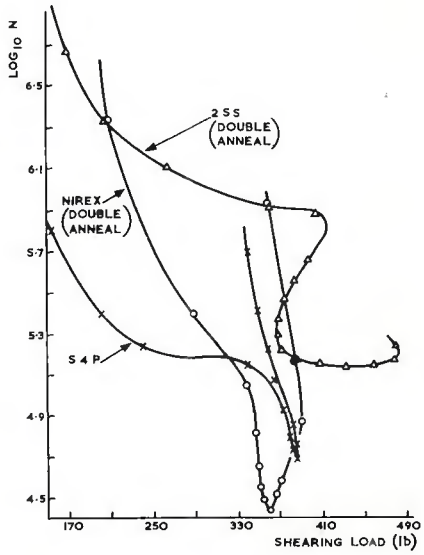

Fig. 6 — Number N of MnS particles/mm² on fracture surfaces versus shearing load

which failure would occur in these materials. However, Fig. 6 shows that a high weld strength can be maintained with relatively large numbers of reprecipitated sulfides. This suggests that the increased alloying due to a larger scale of diffusion counteracts the effect of the increased number of harmful reprecipitated sulfides.

Conclusions

1. The values of weld strength obtained from a simple shear test show that there is an initial rapid increase of strength with increasing input energy from a threshold value of about 600 energy units at transformer tapping 5 for all the nickel base materials. Weld strength remains at a high level for an energy band width of at least 125 units and then rapidly falls away.

2. The fractures obtained in the shearing test correspond to those ob-

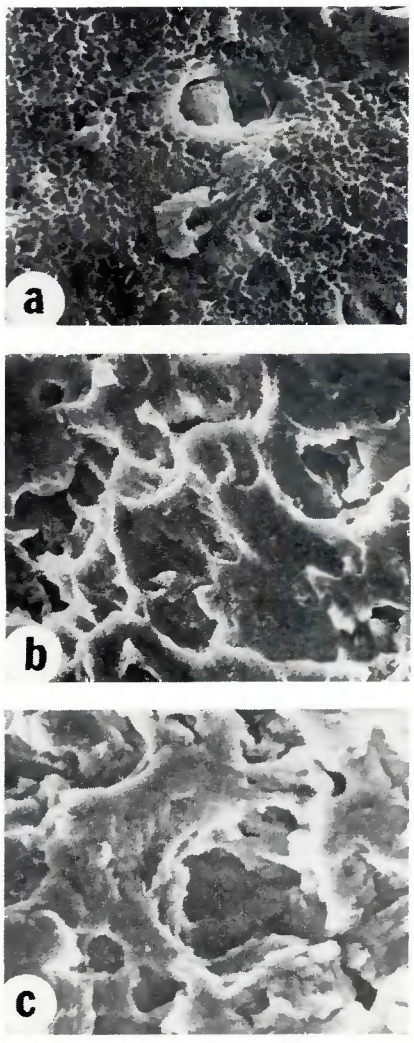

Fig. 7 — Scanning electron photomicrographs showing the change in fracture characteristics for increasing weld input energies of 600, 640, 720 and 760 units (a) to (e) respectively, X2500, not reduced

tained from the initial crude test, and were of the types 'hot-stick', 'body pull-out', 'nickel base failure' and 'weld-line' failure in order of increasing energy inputs.

3. 'Body pull-out' and 'nickel base wire' failures were attributable to, and initiated by, the presence of manganese sulfide particles in the body steel, and the precipitation of iron-titanium carbosulfide respectively.

4. The number of MnS precipitates at the fracture surfaces varied In approximately parabolic manner with welding input energy.

5. The degree of interdiffusion between the elements in the nickel based materials and the free machining steel, and the number of MnS particles per unit area, determine the weld strength. Low particle counts give strong welds provided sufficient interdiffusion has taken place.

6. Generally speaking all the nickel based materials behaved similarly but the results showed that welds made from normal annealed Nirex were of better quality than those welded with the doubly annealed Nirex. On the other hand normal annealed 2S5 welds proved inferior to those produced with doubly annealed 2S5. Both these alloys were found to be capable of producing higher strength welds than with the S4P material.

Acknowledgments

The authors wish to acknowledge the willing assistance obtained from Smiths Industries LImited and Mr. G. France of the University of Salford for their help in the use of automatic welding machines and electron microscopy respectively.

References

1. Hanson, M., *Constitution of Binary Alloys,* McGraw-Hill 2nd Ed. 1958 and 1st supp. 1965.

2. Muan, A. and Osborn, E. F., *Phase Equilibrium Among Oxides in Steel Making,* Addison-Wesley, Reading. Mass. 1965.

3. Sims, C. E., Trans AIME 215. 1959. p. 367.

4. Kiessling, R. and Lange, N., "Non metallic inclusions in steel" J.I.S.I. Pub. No. 100. London 1966.

5. Baker, T. J. and Charles, J. A., "Morphology of Manganese Sulphide" J.I.S.I. Sept. 1972, pp. 702-706.

6. Klessling, R. and Westman, C., J.I.S.I. 204 1966. pp. 377-379.

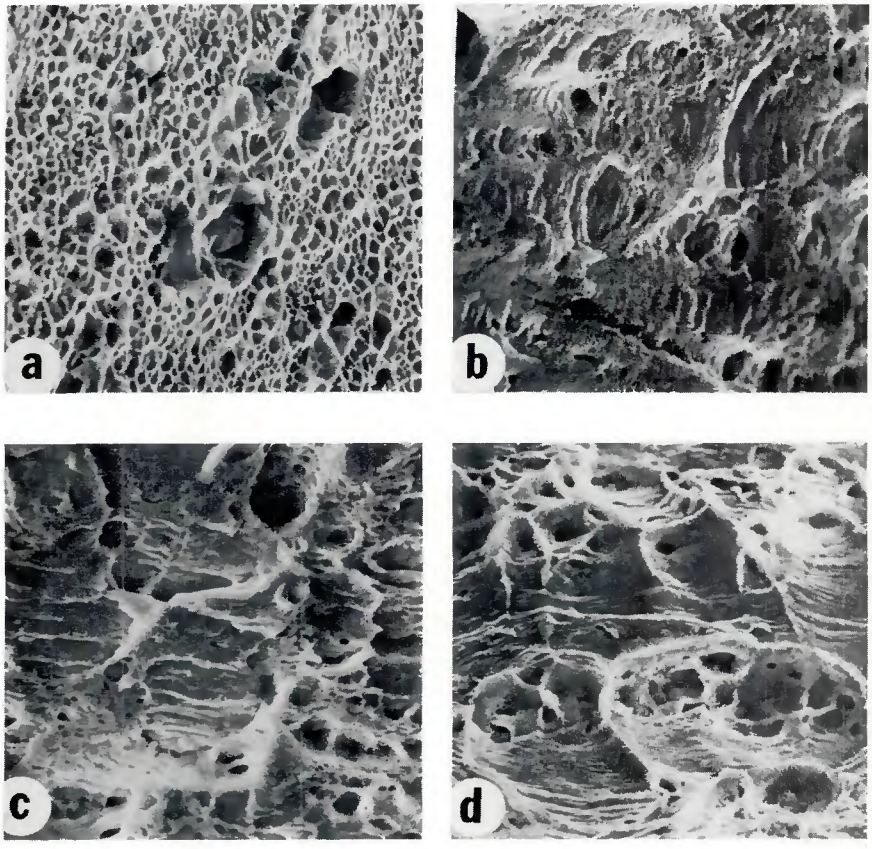

Fig. 8 — Scanning electron photomicrographs of fracture surfaces for 2S5 alloy: (a) and (b) single and double annealed low input energy; (c) and (d) single and double annealed high input energy. X3000, not reduced